Magnetic and electronic properties of CeCo₂ studied by synchrotron radiation

C. L. Dong[1,2,5]**, C. L. Chen**[1,2]**, K. Asokan**[3]**, Y. Y. Chen**[1]**, P. C. Chen**[1]**, Y. S. Liu**[2]**, J. L. Chen**[2]**, C. L. Chang**[*,2]**, H. J. Lin**[4]**, J. F. Lee**[4]**, and J.-H. Guo**[5]

[1] Institute of Physics, Academia Sinica, Taipei 11529, Taiwan, R.O.C.
[2] Department of Physics, Tamkang University, Tamsui 251, Taiwan, R.O.C.
[3] Inter University Accelerator Centre, Aruna Asaf Ali Marg, New Delhi-110067, India
[4] National Synchrotron Radiation Research Center, Hsinchu, Taiwan, R.O.C.
[5] Advanced Light Source, Lawrence Berkeley National Laboratory Berkeley, CA 94720, USA

The magnetic and electronic properties of CeCo₂ bulk and nanoparticles have been investigated using element-specific techniques, X-ray absorption spectroscopy (XAS) and X-ray magnetic circular dichroism (XMCD). The results of Ce L_3-edge XAS spectra shows a higher spectral weight of $4f^1$ configuration in nanoparticles with respect to the bulk, which indicates that the valence of Ce is decreased in nanoparticles. In addition, spectroscopic results from the XMCD at Co $L_{2,3}$-edges and Ce $M_{4,5}$-edges indicate that CeCo₂ undergoes a nonmagnetic to magnetic transition with size reduction. The variations in electronic and magnetic properties of nanoparticles were attributed to the charge transfer related to the sample dimension.

1 Introduction

The extraordinary magnetic and electronic properties of rare-earth compounds are due to the unique nature of *f* electrons, which can possess both localized and band-like characters [1]. One of the interesting properties is the disappearance of the magnetic moment in the *4f* shell under pressure. A recent study of heavy fermion compound CeAl₂ demonstrated that the bulk sample exhibits magnetic ordering whereas the nanoparticle sample is nonmagnetic [2]. The variation of the magnetic properties is attributed to the formation of the nonmagnetic tetravalent Ce with $4f^0$ configuration, which is caused by the higher surface to volume ratio in nanoparticles. On the contrary, bulk CeCo₂ is characterized as a Pauli paramagnet, both Ce and Co are essentially nonmagnetic. However, it undergoes a nonmagnetic to magnetic transition with size reduction [3]. It is of interest to study how the magnetic and electronic properties of CeCo₂ are affected as the sample size is reduced. Our study is based on XAS and XMCD measurements using synchrotron radiation.

2 Experimental

Bulk CeCo₂ was prepared by arc melting the high-purity constituent elements Ce (99.95%) and Co(99.95%) in 1:2 atomic ratios in an argon atmosphere (99.999%). The structure and phase purity were confirmed by X-ray diffraction (XRD) and exhibits cubic Laves structure with a lattice constant $a_0 =$

* Corresponding author: e-mail: clchang@mail.tku.edu.tw, Phone: +886 2 2620 9076, Fax: +886 2 2620 9917

7.160 Å. Nanoparticles of $CeCo_2$ were then fabricated by laser ablation with adjustable laser power under various helium atmospheres. There was no trace of oxide or impurities examined by XRD within the phase resolution (< 3%). The morphology and size of nanoparticles were determined by high-resolution transmission electron microscopy (HRTEM). The diameter of the nanoparticles is about 24 nm. The details of the sample preparation and characterization of the samples have been reported elsewhere [3]. X-ray absorption studies were performed at 17C and 11A beam lines, respectively, around Ce L_3-edge and Ce (Co) $M_{4,5}$- ($L_{2,3}$-) edges in NSRRC, Taiwan. The XMCD were measured at 11 A beam line, spectra were obtained by applying a magnetic field ~1 T at 20 K.

3 Results and discussion

XAS at rare earth L_3-edge has been proven to be a powerful technique for studying the mixed-valence materials [4]. Figure 1(a) displays the Ce L_3-edge XAS for $CeCo_2$ bulk and nanoparticles. The large number of unoccupied Ce *5d* orbital produces (via *2p* to *5d* transition) a prominent white line (A_1) corresponding to $4f^1(5d6s)^4$ (Ce^{3+}) final states. The additional feature at higher energy (B_1) is due to the transition to $4f^0(5d6s)^5$ (Ce^{4+}) final states. The curve fitting for the XAS of bulk sample is shown at the bottom of Fig. 1(a). The feature corresponding to each final state is decomposed into two components, a Lorentian curve and an arctangent step function [5]. The average Ce valence *v* can be estimated by the method described in Ref. [5], $v = (3I_3+4I_4)/(I_3+I_4)$, where I_3 and I_4 represent the integrated intensities of the Lorentians corresponding to Ce^{3+} and Ce^{4+} features respectively. The Ce valence for bulk $CeCo_2$ is estimated to be 3.30, indicating that the bulk $CeCo_2$ is a strongly mixed-valent compound with no local magnetic moment as expected. The estimated Ce valence for nanoparticle sample is 3.22, which is in the intermediate mixed valent regime and should possess local moment [6]. Our valence estimations are in line with the estimations of Ce^{3+} fraction based on heat capacity measurements [7].
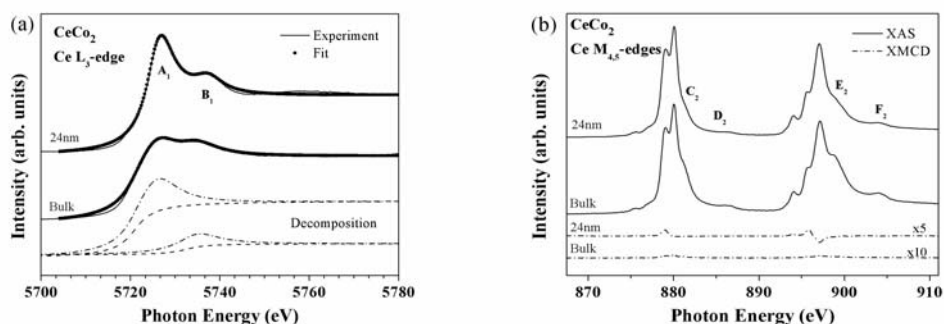

Fig. 1 (a) Ce L_3 XAS and (b) Ce $M_{4,5}$ XAS (solid line) and XMCD (dash) for bulk and 24 nm $CeCo_2$.

The magnetic properties are further investigated by the Ce $M_{4,5}$-XAS and XMCD spectra, e.g., I_+-I_-, are shown in Fig. 1(b). The $I_+(I_-)$ is the absorption spectrum with the photon spin parallel (anti-parallel) to the direction of the magnetic field. The XAS of bulk and nanoparticles are characterized by mixed-valence due to the notable intensities at C_2, D_2, E_2, and F_2, which refer to the tetravalent Ce. A closer inspection of branching ratio (BR) (BR is defined as $I(M_5)/[I(M_4)+I(M_5)]$) [8], which can be also used to study the number of electrons occupying the *f* shell and hence the valence state apart from L_3-edge, gives higher value in nanoparticles (~0.41) than that in bulk (~0.38). This indicates that the enhancement of the *4f* occupation number due to the less hybridization between the *4f* levels with the conduction band which occurs in nanoparticles. The Ce in bulk $CeCo_2$ do not show XMCD signal implying a nonmagnetic ground state. On the other hand, the prominent XMCD signal in nanoparticles indicates that the Ce *4f* electrons possess magnetic moments. No negative peak found in the XMCD spectrum at M_5-edge is a result of the mixture of $4f^0L$ and $4f^1$ (J = 5/2) ground states (where *L* indicates an electron in the conduct-

ing band) through the experimental and theoretical studies [9]. The absent $J = 7/2$ contribution would give rise to higher BR value [9]. This result, again, confirms that the Ce valence is decreased in nanoparticles.

The XAS at Co K-edge reflects mainly the dipole transition from $1s$ to $4p$ states above the Fermi level, as shown in Fig 2(a). The variation of the spectral shape has been pointed out as a fingerprint of hybridization modified due to the electronic perturbation of density of states (DOS) [10]. The change in the intensities at the shoulder-like feature A$_2$ is due to the variation of density of $3d$ unoccupied states through s-p-d hybridization [11]. The reduction of the feature A$_2$ evidences the less hybridization between Co $3d$ states and Ce $4f5d$ conduction states. Since the strong electronic perturbation of the DOS, the $3d$ occupancy number evaluated by feature A$_2$ is suspicious and unfeasible. To straightforwardly probe the unoccupied 3d states, we turn to the Co $L_{2,3}$-edges.
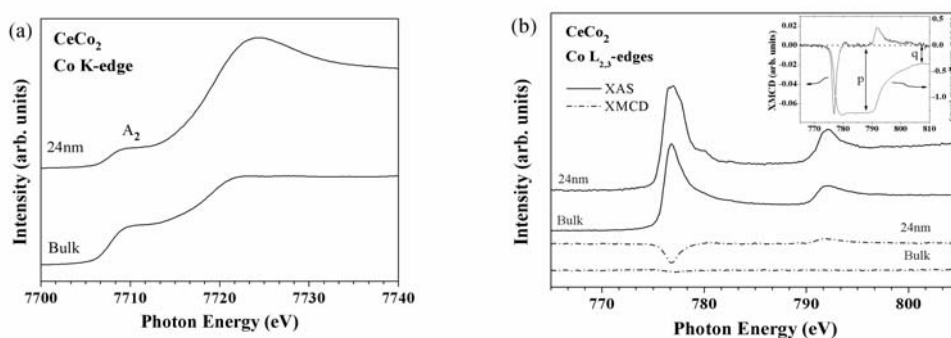
Fig. 2   (a) Co K XAS and (b) Co $L_{2,3}$ XAS (solid line) and XMCD (dash) for bulk and 24 nm CeCo$_2$. The inset in (b) shows the XMCD integrated value of 24 nm CeCo$_2$.

Figure 2(b) shows the Co $L_{2,3}$ XAS spectrum of the CeCo$_2$ bulk and nanoparticles. Rather complicated spectra were observed in nanoparticles. These multiple fine structures may be due to the superposition of Co^{3+} involvement [12]. Similar result was also observed in the hybridized state in Co-Al interface and it is ascribed to the covalent character [13]. It is noted that the unoccupied Co $3d$ state is increased in nanoparticles. Thus the charge transfer between Ce and Co is manifested as a result of dimensional change. The role of Co in CeCo$_2$ magnetic property is given by XMCD also included in the bottom of Fig. 2(b). The XMCD signal of bulk CeCo$_2$ is insignificant indicating Co presents a nonmagnetic ground state. On the other hand, the XMCD signal of the 24 nm nanoparticles shows a prominent negative (positive) amplitude at L_3 (L_2)-edge, which indicates a nonmagnetic to magnetic transition due to the reduced sample dimension. It is, therefore, necessary to take the possibility of the Co impurity or the CoO contamination into account although it is absent in XRD [3]. In principle, the orbital and spin magnetic moment can be estimated by the XMCD sum rule [14]. Due to the uncertainty with the hole number (n_h) of Co $3d$ orbital, the ratio of the orbital to spin magnetic moment can be derived as $m_L/m_S=2q/(9p-6q)$, which is independent of the $3d$ hole number. Here p (q) represents the integrated value over the L_3 (L_3+L_2) range and the magnetic dipole term (T_z) is expected to be very small for the cubic symmetry and can be neglected [15]. The ratio is then estimated to be ~0.05, which is lower than the bulk Co (~0.08) [16] and much reduced compared to that of Co impurities (~0.1±0.02) [17] or other nanostructure system [16, 18]. It has been also pointed out that the decrease of the dimensionality will increase the ratio of the orbit to spin magnetic moment in Co system from either experimental or theoretical aspects [19, 20]. CoO is anti-ferromagnetic and does not contribute to the XMCD spectra. Thus, the magnetic contribution of Co in CeCo$_2$ is unlikely to be originated from the pure Co impurity and it is thus the intrinsic property.

The DOS at the Fermi level comes essentially from the Ce $4f$ and Co $3d$ electrons. The electronic structure at E_F is superposed by a strong Ce $4f$-Co $3d$ hybridization [21]. The electron transfer out of Ce

4f orbital leads to the Ce valence in bulk $CeCo_2$ to be about ~3.3. The Ce *4f*-Co *3d* hybridization strength is reduced in nanoparticles due to the narrower Ce *4f* band width, which is related to the line width of Ce L_3-edge XAS [6]. The line width of feature A_1 in Fig. 1(a) is 8 eV for the bulk sample and 5.9 eV for the nanopaticles. The reduced line width is also observed in feature A_2. The weaker hybridization may be responsible for the decrease of Ce valence to ~3.22 in nanoparticles. The reduction of charge transfer to the Co *3d* band would give rise to the increase of Co magnetic moment [22]. The generalized gradient approximation (GGA+U) and local spin density approximation (LSDA) also predict, in nanostructure system, the Co *3d* state becomes narrower and moves up slightly towards the E_F, and correspondingly increase the DOS at the E_F [19, 23]. As a result, the increase of the spin magnetic moment is expected. Likewise, an enhancement of the orbital moment is also expected due to its higher sensitivity to the crystal field which is generally changed by the atomic coordination [19]. In brief, the electronic structure is altered by the reduced sample dimension and hence the magnetic property is changed.

4   Conclusions

The comparison of the XAS and XMCD allows one to explore the variation of both the charge state and the magnetic moment. As the values of the spin and orbital moments could be drawn separately in this study, it has been found that in $CeCo_2$ nanoparticles the local moment is contributed by both Ce and Co. And such element-specific magnetic information cannot be obtained from a standard magnetometer measurement. Our results indicate the change of the valence is due to the charge transfer between Co and Ce. The variation of the electronic structure gives rise to the different magnetic property. The reduced sample dimension is found to be responsible for these consequences.

References

 [1] L.M. Falicov et al. (Eds.), Valence Fluctuations in Solid (North-Holland, Amsterdam, 1981).
 [2] Y.Y. Chen, Y.D. Yao, C.R. Wang, W.H. Li, C.L. Chang, T.K. Lee et al., Phys. Rev. Lett. **84**, 4990 (2000).
 [3] C.R. Wang, Y.Y. Chen, Y.D. Yao, C.L. Chang et al., J. Magn. Magn. Mater. **239**, 524 (2002).
 [4] G. Liang and M. Croft, Phys. Rev. B **40**, 361 (1989).
 [5] O. Isnard. S. Miraglia, R. Welter, and B. Malaman, J. Synchrotron Radiat. **6**, 701 (1999).
 [6] R.A. Neifeld, M. Croft, T. Mihalisin, C.U. Segre, M. Madigan et al., Phys. Rev. B **32**, 6928 (1985).
 [7] Y.Y. Chen, C.R. Wang, Y.D. Yao, M.N. Ou, and B.J. Chen, submitted to Phys. Rev. Lett.
 [8] M. Finazzi, Ph. Sainctavit, A.-M. Dias, J.-P. Kappler, G. Krill et al., Phys. Rev. B **55**, 3010 (1997).
 [9] M. Finazzi, F.M.F. de Groot et al., J. Electron Spectrosc. Relat. Phenom. **78**, 221 (1996)..
[10] J. Chaboy, A. Marcelli, and L. Bozukov, J. Phys.: Condens. Matter **7**, 8197 (1995).
[11] T.K. Sham, A. Hiraya, and M. Watanabe, Phys. Rev. B **55**, 7585 (1997).
[12] F.M.F. de Groot, J.C. Fuggle, B.T. Thole, and G. A. Sawatzky, Phys. Rev. B **42**, 5459 (1990).
[13] T. Xie, A. Kimura, S. Qiao, T. Moko, J. Muro et al., J. Phys.: Condens. Matter **16**, S5783 (2004).
[14] B.T. Thole, P. Carra, F. Sette, and G. Van der Laan, Phys. Rev. Lett. **68**, 1943 (1992).
[15] C.T. Chen, Y.U. Idzerda et al., Phys. Rev. Lett. **75**, 152 (1995).
[16] U. Wiedwald, M. Spasova, E.L. Salabas, M. Ulmeanu et al., Phys. Rev. B **68**, 064424 (2003).
[17] M. Sargolzaei, I. Opahle et al., J. Magn. Magn. Mater. **290**, 364 (2005).
[18] J.A. Dürr et al., Phys. Rev. B **59**, R701 (1999).
[19] P. Gambardella et al., Nature **416**, 301 (2002).
[20] M. Komelj, C. Ederer, J.W. Davenport, and M. Fähnle, Phys. Rev. B **66**, 140407 (R) (2002).
[21] A.S. Pandilov et al., Physica B **319**, 268 (2002).
[22] T. Yonamine, A.P.B. Tufaile, J. Vogel, A.D. Santos et al., J. Magn. Magn. Mater. **233**, 84 (2001).
[23] G.Y. Guo, Y.K. Wang, and Y.Y. Chen, J. Magn. Magn. Mater. **272-276**, e1193 (2004).